Experimental Research

INTERNATIONAL JOURNAL OF SURGERY

OPEN

Creation of a decellularized vaginal matrix from healthy human vaginal tissue for potential vagina reconstruction: experimental studies

Jayson Sueters, MSc[a], Fangxin Xiao, MSc[d,e,g], Jan-Paul Roovers, MD, PhD[b], Mark-Bram Bouman, MD, PhD[c], Freek Groenman, MD, PhD[b], Huub Maas, PhD[c,d], Judith Huirne, MD, PhD[a], Theo Smit, PhD[a,f,*]

Background: When a disorder causes the absence of a healthy, full-size vagina, various neovaginal creation methods are available. Sometimes dilation or stretching of the vaginal cavity is sufficient, but intestinal or dermal flap tissue is generally required. However, different inherent tissue properties cause complications. Therefore, a lost body part should be replaced with a similar material. The use of organ-specific acellular vaginal tissue carries great potential, as its similar architecture and matrix composition make it suitable for vaginal regeneration.

Methods: The authors developed an optimized protocol for decellularization of healthy human vaginal tissue. Resected colpectomy tissue from 12 healthy transgender patients was used. Successful decellularization was confirmed by applying acellular criteria from in-vivo remodeling reports. Suitability as a tissue-mimicking scaffold for vaginal reconstruction was determined by visible structural features, biocompatibility during stretching, and the presence of visible collagen, elastin, laminin, and fibronectin.

Results: Histological examination confirmed the preservation of structural features, and minimal cellular residue was seen during fluorescence microscopy, DNA and RNA quantification, and fragment length examination. Biomechanical testing showed decreased peak load (55%, $P < 0.05$), strain at rupture (23%, $P < 0.01$), and ultimate tensile stress (55%, $P < 0.05$) after decellularization, while the elastic modulus (68%) did not decrease significantly. Fluorescence microscopy revealed preserved Fibronectin-I/II/III and Laminin-I/II, while Collagen-I and Ficolin-2B were decreased but mostly retained.

Conclusions: The absence of cellular residue, moderately altered biomechanical extracellular matrix properties, and mostly preserved structural proteins appear to make our decellularized human vaginal matrix a suitable tissue-mimicking scaffold for vagina transplantation when tissue survival through vascularization and innervation are accomplished in the future.

Keywords: acellular biomaterial, acellular vaginal tissue, decellularization, tissue engineering, vagina reconstruction

[a]Department of Gynaecology, Amsterdam Reproduction and Development, [b]Department of Obstetrics and Gynecology, Amsterdam Reproduction and Development, [c]Department of Plastic, Reconstructive and Hand Surgery, Amsterdam UMC – location VUmc, [d]Department of Human Movement Sciences, Faculty of Behavioral and Movement Sciences, Vrije Universiteit Amsterdam, [e]AMS – Musculoskeletal Health, Amsterdam Movement Sciences, VU Research Institutes, [f]Department of Medical Biology, Amsterdam UMC – location AMC, Amsterdam, The Netherlands and [g]School of Exercise and Health, Shanghai University of Sport, Shanghai, China

Sponsorships or competing interests that may be relevant to content are disclosed at the end of this article.

*Corresponding author. Address: Amsterdam University medical Centers, Meibergdreef 9, 1085 AZ Amsterdam, the Netherlands. Tel.: +31 205 667 696. E-mail: th.smit@amsterdamumc.nl (Theo Smit).

International Journal of Surgery (2023) 109:3905–3918

Received 26 June 2023; Accepted 21 August 2023

Supplemental Digital Content is available for this article. Direct URL citations are provided in the HTML and PDF versions of this article on the journal's website, www.lww.com/international-journal-of-surgery.

Published online 26 September 2023

http://dx.doi.org/10.1097/JS9.0000000000000727

Background

Absence of a functional vagina is caused by various medical disorders of congenital [Mayer–Rokitansky–Küster–Hauser syndrome (MRKHS), cloacal malformations, endocrine abnormalities, gender dysphoria, and disorder of sex development] or acquired origin (like cancer and trauma), that tremendously reduce the quality of life and psychological well-being[1]. This often requires partial or total reconstruction, aiming to construct a vagina with function and sensation similar to that of a native vagina. Vaginoplasty is mostly performed on patients with MRKHS or Male-to-Female Gender Dysphoria (MtF GD). MRKHS presents as congenital aplasia of the uterus and upper two-thirds of the vagina with normal secondary sexual characteristics, with ~1 : 5000 prevalence in genotypical females[2]. Nonsurgical alternatives carry great disadvantages[3,4] and regularly require secondary surgical treatment([5]. Expression of GD, an incongruency between assigned sex at birth and gender, is diverse, with a global prevalence of 1 : 2900–45,000 in individuals assigned male at birth[6]. Feminizing genital gender assignment surgery is not always desired by the patient, but roughly 5–20% undergo a vaginoplasty globally to increase quality of life and sexual function[7,8]. Additional flaps are regularly required due to insufficient local,

autologous skin volume due to puberty hormone blockers at an early age[9,10].

For vaginoplasty, over 20 flap-based approaches with characteristic (dis)advantages have been developed without a golden standard[11,12]. Allogenic and xenoflaps pose high risk of immunorejection[12], xenoflaps also carry a cross-species transmission risk of infections and diseases[13]. Therefore, vaginoplasty generally relies on autologous dermal or intestinal flaps, but heterotopic vagina-mimicking flaps are inherently different in physiology[14] (and grafts even more so). Consequent lack of or excessive vaginal mucus production, esthetic issues, and inadequate neovaginal lengths regularly require revisional surgery[15,16]. Hence, vaginoplasty outcomes are not always satisfactory, with substantial room for improvement.

Tissue engineering offers a great alternative, as it can theoretically create any tissue or organ through infinite combinations of three essentials: 1) cells (type and state), 2) biomaterial (composition, mechanical properties, texture, and condition), and 3) signaling factors (e.g. growth factors and bioreactors)[17]. Tissue-engineered organs have found successful clinical applications[18,19], with decellularized cartilage, bone, tendon, heart, lung, vessel, skeletal muscle, intestine, liver, pancreas, kidney, bladder, cornea, and uterus. This field is challenging due to infinite tunability, but current in-vitro cultured neovaginal constructs offer great promise for autogenic flaps without large donor site harvesting and associated risks[20].

We previously reviewed tissue engineering applications for vaginoplasty[17]. Most included articles only reporting in-vitro experiments or small transplants in rodents. In clinically relevant sizes (centimeter-range and larger), tissue survival is restricted by diffusion and mass transport of nutrients. Mass transport is also crucial directly after implantation, as a vascular network is not established yet. Constructs of clinically relevant sizes mostly incorporated extracellular matrix (ECM) biomaterials, reconstructed partial vaginas[21] and applied cell-free grafts or flaps[22]. Clinical trials reported granulation, bacterial infections, and inflammation in cell-free scaffolds[22,23], whereas autologous cells reduced fibrosis and increased regeneration and satisfactional with complication-free results[24].

In theory, vaginal matrices form the ideal biomaterial to prevent complications from inherent physiological differences. An acellular vaginal matrix (AVM) from rats[25,26] or pigs[27] has been tested and even transplanted in rats[23,25,26]. Partial, cell-free AVM constructs resulted in adhesion without chronic inflammation or fibrosis and good biomechanical properties, biocompatibility, and the presence of various growth factors[23,26]. Despite successful isolation of human vaginal epithelial cells, vaginal stromal cells, vaginal fibroblasts, and vaginal mucosa, human AVM has only been created once from pelvic organ prolapse patients[28].

In our medical center, colpectomy was performed 60 times in 2022 in female-to-male (FtM) transgender patients, to reduce vaginal discharge or to prevent fistula formation in urethral lengthening for phallo- or metaidoioplasty[29]. Our aim was to use resected colpectomy tissue to create human decellularized vaginal matrix. Remnant cellular material within ECM may cause cytocompatibility issues and adverse host responses *in vivo*[30] above (unknown) threshold concentrations. Based on in-vivo remodeling reports, the following criteria suffice to assess successful decellularization (1): No nuclear material visible (2), less than 50 ng OR less than 10% dsDNA/mg ECM dry weight, and (3) DNA fragments less than 200 base pair[31]. To assess functionality, three criteria were added. Avoidance of chemically induced structural damage, was defined as (4): visible structural features. Furthermore, elasticity is a predominant feature of the vagina that allows elongation during intercourse and passage of a full-term baby during birth, this was investigated by (5): biocompatibility during stretching. Lastly, vaginal characteristics greatly depend on interaction between cells, the ECM, and its various structural proteins; thus, biocompatibility was further investigated by (6): presence of visible collagen, elastin, laminin, and fibronectin.

HIGHLIGHTS

- We developed an optimized decellularization protocol for human vaginal tissue from healthy, full human donor flaps.
- The resulting acellular vaginal matrix (AVM) was free from chemically induced damage, as structural features were retained.
- Successful decellularization was confirmed by low DNA (and RNA) quantity and small DNA base pairs size (according to guidelines for acellular biomaterials).
- The AVM showed decreased biomechanical properties but comparable behavior for daily activity-like conditions.
- The AVM showed partial retention of constituent extracellular matrix proteins.
- This tissue-mimicking scaffold needs further improvements to address tissue functionality and survival, which is part of our current follow-up study.

Methods

Patients and surgical procedure

Vaginal tissue was retrieved from 12 patients (Fig. S1, Supplemental Digital Content 1, http://links.lww.com/JS9/B61) during robotic-assisted laparoscopic colpectomy between April 2022 and December 2022. All procedures were performed with the daVinci XI system (Intuitive, Madrid, Spain) (Fig. S2, Supplemental Digital Content 2, http://links.lww.com/JS9/B62). First, the vaginal epithelium was carefully dissected with monopolar scissors and fenestrated the bipolar forceps to prevent bleeding as much as possible[32]. A dissection was performed ~2 cm proximal of the ostium urethrae externum (marked by a suture) and up to the posterior commissure level[32]. Vaginal tissue (from the epithelium, lamina propria, and smooth muscle layers) was removed. The adventitia was preserved to prevent nerve injury to adjacent structures, fistula to the bladder, urethra, or rectum and bleeding from the perivaginal plexus[32]. Per patient, two mesoderms and an ectoderm ring were obtained. The vaginal apex was sutured laparoscopically by suturing the endopelvic fascia of the vesicovaginal space and remnants of the rectovaginal septum together[32]. If necessary, residual introital epithelium was removed vaginally, and the introitus was narrowed through the approximation of bulbocavernosus muscles with 1–2 sutures[32]. Vaginal tissue was directly stored in PBS with pH 7.4 on ice until decellularization was initiated. Written informed consent for the experimental use of resected vaginal tissue was obtained from all patients. Tissue collection and experimental usage were approved by the institutional Medical Ethical Examination Committee.

Decellularization

Decellularization is commonly based on chemical, biological, and/or physical processes, depending on tissue origin, size, and type[31]. Our DC protocol excluded physical processes to prevent ECM disruption[31] and was derived from documented protocols for whole, large organ vaginal tissue[20,23,28]. We applied Triton X-100, Sodium deoxycholate, and DNase I at minimally required concentrations, to prevent diminished growth factors, proteins, mechanical properties, and ultrastructure[31]. Detrimental effects on ECM were minimized by keeping maximum exposure time to reagent under 24 h[31]. Decellularization was started within 4 h after surgical tissue removal. Decellularization is initiated by 24 h incubation at 37°C with constant agitation (100 motions/min) in 0.18% w/w Triton x-100 (Sigma-Aldrich, St. Louis, Missouri, USA) and 0.05% w/w sodium deoxycholate (Sigma-Aldrich) in PBS (Fresenius Kabi, Zeist, Utrecht, The Netherlands). Tissue was washed 20 min in PBS twice and washed 72 h at 4°C with constant agitation (on a roller) in PBS with 1 U/ml penicillin and 1 µg/ml streptomycin (Life Technologies Europe BV, Bleiswijk, Zuid-Holland, The Netherlands). Next, enzymatic digestion involved 24 h incubation at 37°C by 150 IU/ml DNase I (Sigma-Aldrich) and 50 mmol $MgCl_2$ (Sigma-Aldrich) in PBS. Before further processing, 24 h incubation at 4°C with constant agitation in 1 U/ml penicillin and 1 µg/ml streptomycin diluted in PBS was performed, followed by an extensive PBS wash. The total protocol duration was 6 days.

Embedding by semiautomated tissue processing

Tissues were embedded in the Epredia Excelsior AS Tissue Processor (Thermo Fisher Scientific, Landsmeer, Zuid-Holland, the Netherlands). This sequentially involved 1 h in 70% ethanol, 1 h in 90% ethanol, 1 h in 96% ethanol, and (thrice) 1 h in 100% ethanol at RT. Three sequential xylene steps at 37°C, 40°C, and 45°C were performed, followed by sequential paraffin bath 1, 2, and 3 in three steps of each 1 h and 20 min at 62°C. Next, tissue is manually embedded in liquid paraffin of 55°C by 1 h solidification at RT on a cooled plate of – 5°C. After overnight 4°C paraffin wax hardening, samples are ready for microtome sectioning.

DAPI with ethidium bromide or hematoxylin with eosin staining

4',6-diamidino-2-phenylindole (DAPI) and ethidium bromide (EtBr) bind to nuclear cellular material with distinctive binding sensitivity and fluorescence intensity due to inherent differences in binding method. [DAPI (minor groove binder) has a high DNA affinity with high fluorescence intensity, whereas EtBr (intercalator) binding has low fluorescence with high RNA binding affinity]. DAPI- and EtBr-staining combined allows extensive assessment of nuclear cellular material with Blue/Purple-stained dsDNA and Red-stained RNA[33,34]. A DAPI with EtBr staining and hematoxylin with eosin (H&E) staining was performed on native and decellularized vaginal tissue. Samples were fixed overnight at RT with constant agitation (on a roller) in 4% w/v formaldehyde (ROTI Histofix 4%; Carl Roth, Karlsruhe, Mannheim, Germany). Tissue was washed 30 min in PBS, followed by three cycles of 30 min in 70% ethanol (Sigma-Aldrich) at RT. Tissue was embedded according to *Embedding by semi-automated tissue processing* (above). Samples were sliced by a Leica RM2255 microtome (Leica Biosystems, Deer Park, Illinois, USA) to 5 µm-thick sections, using a 6° knife angle. Sections were mounted on microscope slides in a Leica HI1210 water bath (Leica Biosystems) at 37.2°C. The slide-sections were processed by 5 min deparaffinization in xylene (twice), followed by sequential steps of 2 min hydration in 100% ethanol (twice), 96% ethanol and 70% ethanol. Staining involved 5 min incubation at RT in either 0.2 µg/ml DAPI (Sigma-Aldrich) in PBS or 5 min incubation in 1 mg/ml hematoxylin (Sigma-Aldrich) (0.5 g haematoxylin + 25 g aluminum potassium sulphate + 0.1 g sodium iodate + 10 ml glacial acetic acid + 500 ml demi-water), followed by 3 min incubation in 5 mg/ml eosin (Sigma-Aldrich) diluted in 70% ethanol. DAPI-stained slides were embedded with Prolong Gold Antifade Reagent (Life Technologies Europe BV), hardened 1 h at RT and placed at 4°C for several hours before analysis with the Olympus BX 41 (Olympus, Tokyo, Japan) light microscope. H&E-stained slides were embedded with 1× Entellan (Sigma-Aldrich) and dried overnight before inspection with the Leica DM5000B (Leica Biosystems) fluorescence microscope.

Quantitative DNA and RNA analysis

DNA and RNA residues were isolated with a commercial DNeasy Blood and Tissue kit (Qiangen, Shenzhen, Nanshan, China). In brief, a maximum of 25 mg of thawed native or wet DC vaginal tissue was placed in microcentrifuge tubes with 180 µl buffer ATL (Sodium dodecyl sulphate) and 20 µl proteinase K. The tubes were vortexed and placed on a 56°C heated tube-holder plate until complete digestion (~90 mins). During digestion, vortexing was performed with 15 min intervals. Next, lysis buffer AL (Guanidine hydrochloride mixed with maleic acid) in ethanol was added and after 1 min centrifugation at 6000*g*, several washing steps were performed to remove contaminates. The residue mixture was diluted by buffer AE. DNA and RNA concentrations were measured with a Qubit 2.0 fluorometer (Thermo Fisher Scientific). The dsDNA HS Assay kit (Thermo Fisher Scientific) was applied for DNA, with an optimized working solution –DNA sample ratio at 0.1–120 ng/µl application range. The RNA HS Assay kit (Thermo Fisher Scientific) was applied for RNA, with optimized working solution – RNA sample ratio at 4–200 ng/µl application range. The RNA and DNA quantity per mg of dry ECM tissue was calculated.

DNA content analysis

The DNA concentration in DC vaginal tissue was too low for assessment of DNA fragments by gel electrophoresis. Therefore, quantitative DNA analysis was followed by dilution of DNA in PBS to 1 ng/µl and analysis of DNA fragment length with an Agilent 4200 TapeStation System (Agilent Technologies, Amstelveen, Noord-Holland, the Netherlands).

Biomechanical analysis of tensile stress, strain at rupture, and elastic modulus

For biomechanical analysis, wet native or DC vaginal tissue was mechanically loaded with the EBERS TC-3 mechanical stimulation bioreactor (EBERS Medical Technology SL, Zaragoza, Spain). Section dimensions were measured with a vernier caliper. Short strips of $(3.4 \pm 0.5) \times (3.2 \pm 1.2)$ mm [native] or $(3.9 \pm 0.8) \times (3.1 \pm 0.9)$ mm [DC] in width × thickness, were clamped between two flat grips with an initial 5-mm gap. Next, samples were

elongated along bottom-to-top direction with 120 mm/min elongation speed. With 1 mm addition elongation steps, the test was stopped at point of full rupture. Seven biological replicates were tested for each sample condition and averaging over 10 consecutive load cycles was applied. Strain ε was calculated as the percentage of elongation to initial length ratio $= \Delta L/L_0 \times 100\%$[23,35]. Strength F was calculated as the load force as function of elongation and the peak load F_{max} was defined as the maximum strength derived from the $F(\varepsilon)$-plot. Tensile stress σ was calculated from strength F, mean width w and thickness t as $\sigma = F/(w \times t)$. Ultimate tensile strength σ_{ult} was the maximum tensile stress derived from the $\sigma(\varepsilon)$ plot[23,35]. The corresponding strain at σ_{ult} was defined as the strain at rupture ε_{rup} and the elastic modulus E was calculated as: $E = 0.4 \times \sigma_{ult}/(\varepsilon_{60\%\sigma} - \varepsilon_{20\%\sigma})$. Here, strain $\varepsilon_{60\%\sigma}$ and $\varepsilon_{20\%\sigma}$ corresponded to 60 and 20% of ultimate tensile strength σ_{ult}, respectively[23,35].

Biomechanical analysis of intact vaginal rings was tested with a displacement-controlled dynamic testing setup. Vaginal rings were $(27.4 \pm 1.9) \times (4.4 \pm 0.9) \times (2.6 \pm 0.5)$ mm [native] or $(26.1 \pm 3.5) \times (3.8 \pm 0.8) \times (2.9 \pm 0.5)$ mm [DC] in length × width × thickness. Nondissolvable sutures were placed around the ring at two opposite sides. One suture was clamped at a fixed position, whereas the second sutures was connected to a force transducer (ALPHA load beam transducer, 25 N maximum capacity, maximum output error <0.1%, compliance 0.0162 mm/N; BLH Electronics Inc.). This force transducer was mounted on a servomotor (MTS50C-z8; Thorlabs, Cambridgeshire, UK), to generate a pulling force to the tissue by movement at a constant velocity of 6 mm/min and a maximum acceleration/deceleration of 4.5 mm/s^2. Custom LabVIEW (LabVIEW 13.0; National Instruments, Austin, Texas, USA) programs were used for motor movement control and to collect displacement and force signals. Mechanical loading of 10 consecutives cycles was performed at predetermined strains. Force signal was sampled at 1000 Hz, processed through a second order low pass zero-lag Butterworth filter with a cutoff frequency of 5 Hz. The peak load F was determined as previously described.

Immunofluorescence analysis of ECM constitutive proteins

Native and DC vaginal tissue was assessed by immunofluorescence of constitutive ECM proteins. Slides were deparaffinized and rehydrated according to *DAPI with* EtBr *or H&E staining* (above). Next, slides were washed thrice for 5 min in PBS while slowly shaking. For Collagen-I and Ficolin-2B slides, antigen retrieval was performed for 10 min in 10 mmol/l Tris (#10708976001; Roche, Woerden, Utrecht, the Netherlands) + 1 mmol/l EDTA (#161-0770; Bio-rad, Lunteren, Gelderland, the Netherlands) at pH = 9.0. For Laminin- and Fibronectin-slides, quenching of auto fluorescence was performed by 30 s incubation with 1× TrueBlack (#23007; Biotium, Fremont, California, USA) diluted in 70% ethanol, followed by a 5 min washing step in PBS (thrice) while slowly shaking. Laminin- and Fibronectin-slides were further processed to minimize a-specific binding of antibodies by 1 h incubation in a humid slide box at RT with 1× Superblock Blocking Buffer (#37515; ThermoFischer Scientific, Landsmeer, Zuid-Holland, the Netherlands) in PBS. For Collagen-I and Ficolin-2B slides, 1× Superblock Blocking Buffer was replaced by 3% BSA – IgG free (#A0281-5G; Sigma) + 0.1% Tween-20 (#P1379; Sigma) + 0.1% BSAc – IgG free (Sigma). Next, a short and gentle PBS rinse was performed. Slides were incubated with fluorescent conjugated antibodies at 5 µg/ml Fibronectin-I/II/III (#ab198934, rabbit mAb, 1 : 100 concentration, overnight incubation at 4°C; Abcam) and 7.1 µg/ml Laminin-I/II (#PA5-22901, rabbit pAb, 1 : 100 concentration, overnight incubation at 4°C; ThermoFischer Scientific) diluted in Bright Diluent (#UD09-500; VWR, Amsterdam, Noord-Holland, Amsterdam) or 20 µg/ml Collagen-I (#BS-10423R-A350 and BS-0709R-A350, 1 : 50 concentration, overnight incubation at 4°C; Bioss antibodies) and 20 µg/ml Ficolin (#BS-13162R-A594, 1 : 50 concentration, overnight incubation at 4°C; Bioss antibodies) diluted in 3% BSA – IgG free (#A0281-5G; Sigma) + 0.1% Tween-20 (#P1379; Sigma). Next, slides were accumulated 30 min at RT, followed by a 10 min washing step in PBS (thrice) while slowly shaking. Ficolin-, Laminin-, and Fibronectin-slides were incubated for 5 min with 300 ng/mL DAPI in PBS. Collagen-slides were incubated for 15 min with 1 µg/ml EtBr (#A1152.0010; Applichem, Darmstadt, Germany) in PBS. Lastly, all slides were washed 5 min in PBS and embedded with 1× Prolong Gold Antifade Reagent (Life Technologies Europe BV), then hardened for 1 h at RT. Slides were placed at 4°C for a couple of hours prior to analysis with the Olympus BX 41 (Olympus) light microscope.

Statistical analysis

For feasibility, vaginal tissue from 12 patients was obtained to perform experiments with seven biological and three technical replicates per protocol. Statistical analysis was performed on native and decellularized tissue, to identify significant differences in DNA and RNA quantity. The paired *t*-test was applied and results were expressed as mean with SD. Biomechanical experiments were performed with seven biological replicates and 10 repetitive measurements per elongation step. The paired *t*-test was applied and results were expressed as mean with SEM. The *P* value was obtained in a one-tailed test and was considered statistically significant for $*P$ less than or equal to 0.05, $**P$ less than or equal to 0.01, and $***P$ less than or equal to 0.001.

Results

Gross anatomic characteristics of DC vaginal scaffolds

The vaginal wall (Fig. 1A/B) consists of squamous epithelium (epithelial cells), lamina propria (fibroblasts, thin-walled blood vessels), muscularis (smooth muscle cells), and adventitia (blood vessels, lymphatic ducts, nerves). The proximal vagina (mesoderm) originates from paramesonephric duct and distal vagina (ectoderm) from urogenital sinus. Vaginal removal is a delicate procedure due to these thin wall layers. Furthermore, elasticity and coagulation are patient dependent and affected procedure difficulty. Vaginal tissue was successfully removed by dissection as two mesoderm rings and an ectoderm ring (Fig. 1C) per patient or as vaginal tissue with tears (Fig. 1D). Patient mean age at time of surgery was 27.1 (range: 19–51) years with a mean of 5.9 (range: 2–11) years presurgical androgen exposure by either testosterone injection (Nebido; Bayer Healthcare and Sustanon; Aspen) or by testosterone gel (Androgel; Besins Healthcare) (Supplementary S1, Supplemental Digital Content 1, http://links.lww.com/JS9/B61). First, burned and cankered (i.e. ragged, lacerated, or thinned) sections were removed, after which tissue was deemed suitable for analysis. Native tissue was sectioned to less than 25 mg dry weight for storage compatibility. Next, this tissue was either fixed with 70% ethanol at 4°C for microscopic

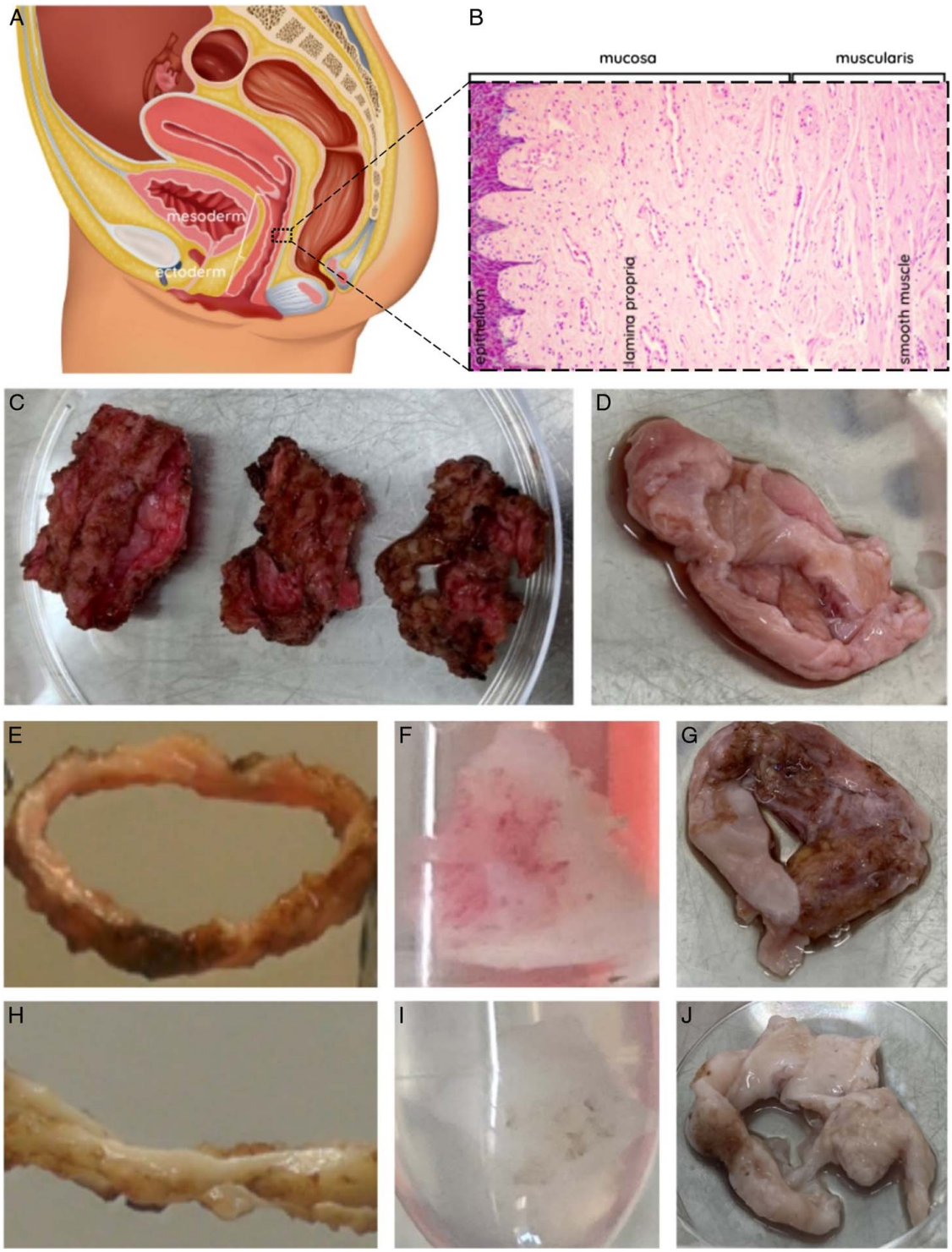

Figure 1. (A) Illustration of female reproductive system sideview with fractions of mesoderm tissue (two-third proximal vagina) and ectoderm tissue (one-third distal vagina). (B) Layers of the vagina wall (left to right): squamous epithelium – lamina propria – smooth muscle – adventitia (not depicted). (C) Completely removed vaginal rings from a single patient during robot-assisted laparoscopic colpectomy. Orientation proximal-distal origin from left to right. Image was taken before removal of burned and cankered tissue prior to the decellularization protocol. (D) Removed vaginal tissue from a single patient during vaginally performed colpectomy. Image was taken prior to the decellularization protocol. Macroscopic inspection of successful decellularization (DC) showed pink vagina before DC in (E) ring, (F), block, and (G) section, and white vaginal tissue after DC in (H) ring, (I) block, and (J) section.

examination of DAPI- and H&E-staining or it was dried and snap-frozen in liquid N_2 with storage at – 80°C before quantitative DNA and RNA analysis. Decellularized vagina rings were sectioned if required for analysis. Decellularization was without issues and could visually be observed by a color-change from pink native (Fig. 1E–G) to white DC tissue (Fig. 1H–J) for all samples. This initially indicates (some or) successful DC. Decellularization consisted of membrane disruption (with 0.18% w/w Triton x-100 and 0.05% w/w sodium deoxycholate in PBS), followed by enzymatic digestion (with 150 IU/ml DNase I and 50 mmol $MgCl_2$ in PBS).

Structural features with no nuclear cellular material visible after DC

DAPI- and EtBr-staining confirmed that positive controls of mesoderm (Fig. 2A) and ectoderm (Fig. 2B) origin contained an abundancy of visible DNA and RNA. Visible DNA and RNA was absent after DC (Fig. 2C). After partial DC by enzymatic digestion (Fig. 2D), visible RNA and the majority of DNA was removed successfully. After partial DC by membrane disruption, DNA and RNA remained visible (Fig. 2E).

H&E-staining confirmed the presence of intact structures and an abundancy of visible nuclei in native mesoderm (Fig. 2A) and ectoderm (Fig. 2B) sections. Structures remained intact and visible nuclei were absent after DC (Fig. 2C). Partial DC by enzymatic digestion (Fig. 2D) caused structural alterations. Partial DC by membrane disruption did preserve structures, but also preserved visible nuclei (Fig. 2E).

Decellularization efficacy was further assessed on full-size vagina wall rings at clinically relevant tissue sizes (Fig. 3). Again, H&E-staining confirmed the presence of intact structures and an abundancy of visible nuclei in native mesoderm rings (Fig. 3A). Visible nuclear components were absent and structures remained intact after DC of mesoderm (Fig. 3B) and ectoderm (Fig. 3C) rings. DC by twice the original chemical concentrations (Fig. 3D) often resulted in compromised structures and tissue became physically difficult to handle, due to extreme softening. Vaginal tissue was not compromised by (long-term) presurgical androgen exposure. No epithelial atrophy (thinned squamous epithelium) or prostatic metaplasia (glandular structures in epithelium or subepithelial stroma) were assessed.

DNA concentration <10% dsDNA/mg dry ECM weight after DC

Analysis of quantitative DNA- and RNA-residue confirmed the removal of nuclear cellular material by DC. DsDNA in vaginal tissue blocks was significantly reduced ($P < 0.001$) below 50 ng and 10% dsDNA/mg dry ECM weight after DC (Fig. 4A). DsDNA was preserved ($P > 0.05$) after partial DC by membrane disruption (Fig. 4A) and RNA was preserved ($0.001 < P < 0.01$) after partial DC by enzymatic digestion (Fig. 4B). This indicates that both enzymatic digestion and membrane disruption are essential to our DC protocol. Addition of 3 U/ml RNase A to the DC process did not significantly reduced RNA (Fig. 4B).

Additional assessment in vaginal tissue rings of clinically relevant sizes, confirmed that dsDNA (Fig. 4C) and RNA (Fig. 4D) were significantly ($P < 0.001$) reduced after DC of mesoderm and ectoderm tissue. DsDNA reduced below 50 ng and 10% dsDNA/mg dry ECM weight. DC by twice the original chemical concentrations did not significantly further reduce dsDNA or RNA.

DNA fragments less than 200 base pairs after DC

Assessment of DNA-residue fragments confirmed that DNA was reduced to lengths below 200 bp after DC (Fig. S3, Supplemental Digital Content 3, http://links.lww.com/JS9/B63). However, when DNase I concentrations were reduced, the DNA fragment

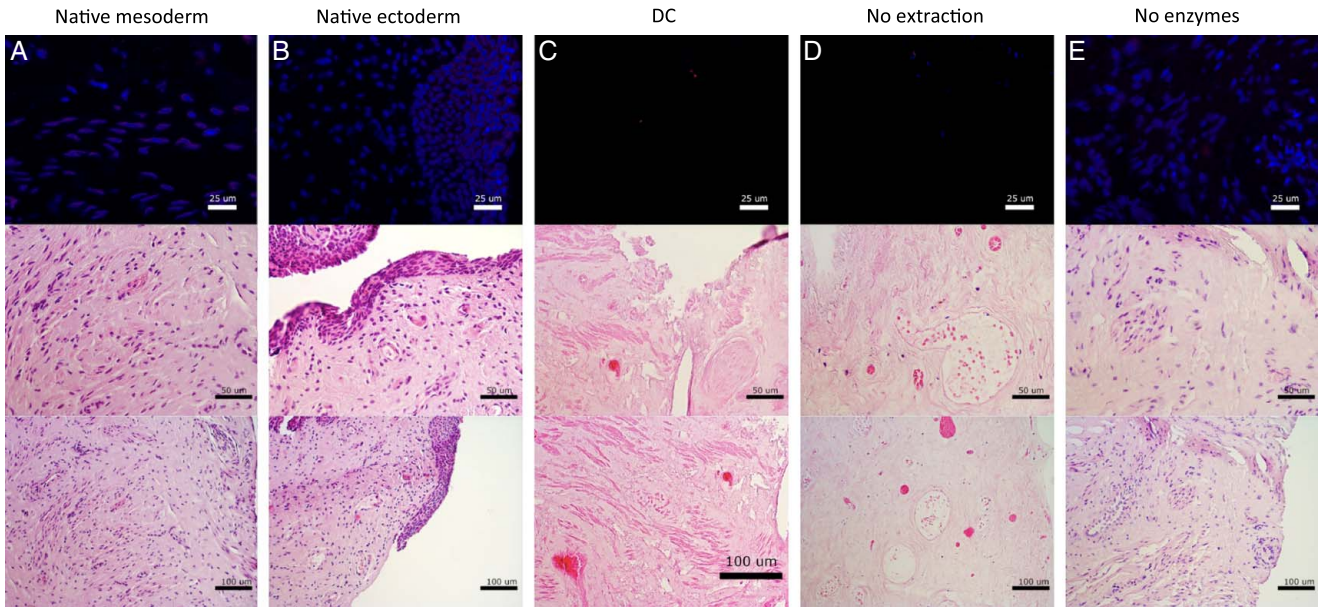

Figure 2. Histological assessment with 4',6-diamidino-2-phenylindole and ethidium bromide staining (top) and assessment of tissue structure with hematoxylin and eosin staining (center and bottom) of (A) native mesoderm, (B) native ectoderm vaginal tissue, (C) decellularization, (D) enzymatic degradation only, and (E) membrane disruption only.

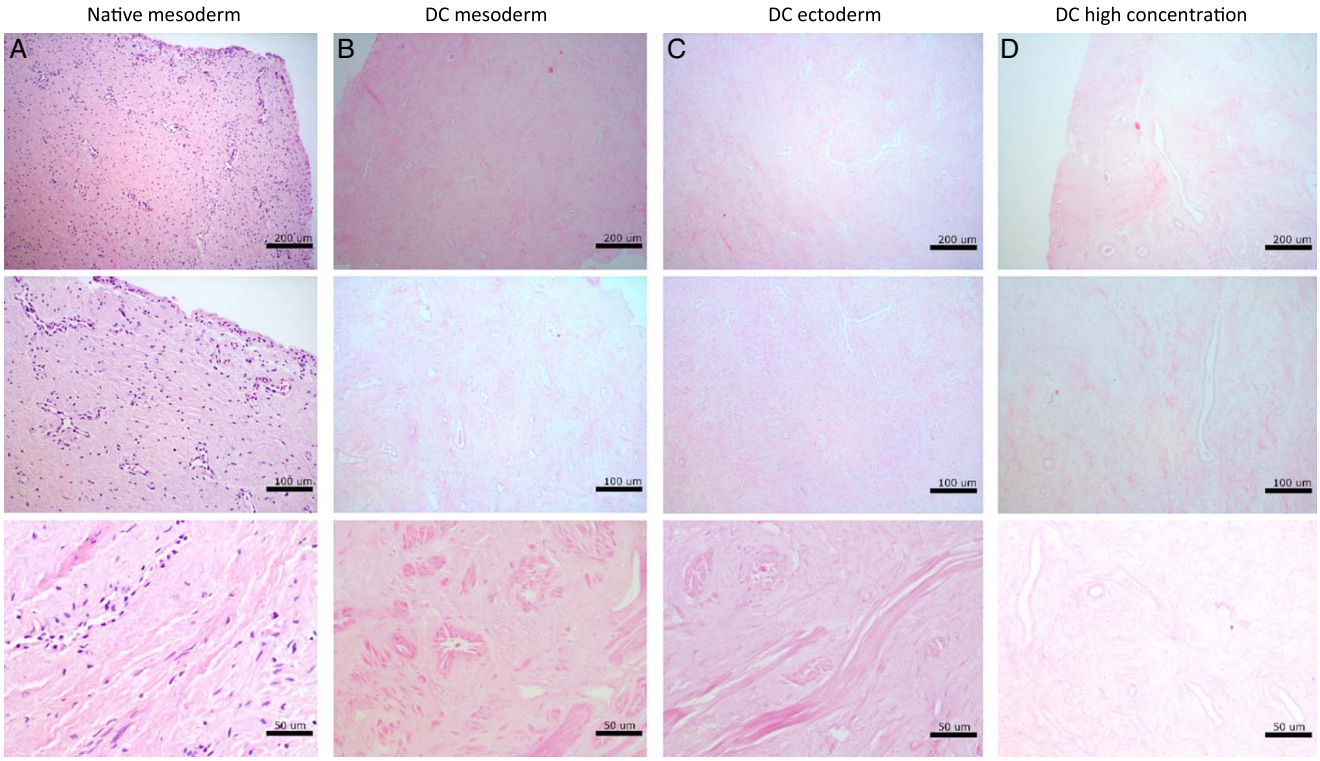

Figure 3. Assessment of tissue structure with hematoxylin and eosin staining of (A) native mesoderm, (B) decellularized mesoderm, (C) decellularized ectoderm, and (D) decellularized mesoderm vaginal tissue at high concentration.

lengths increased. Therefore, a DNase I concentration of 150 U/ml was applied for DC, although 100 U/ml DNase I is sufficient for fragmentation. Partial DC by enzymatic digestion resulted in DNA lengths above 200 bp and partial DC by membrane disruption resulted in DNA fragment lengths below 200 bp.

Decreased strain at rupture, tensile stress, and elastic modulus after DC

Biomechanical analysis in short strips of vaginal tissue confirmed that strength and tensile stress were low and similar for native and DC tissue, until tissue is elongated to twice the initial length ($\varepsilon = 100\%$). This is the point where elastic wall components were stretched and corresponded to a pull strength of 0.63 N with 57.5 kPa tensile stress (Fig. 5A/B). Strength and tensile stress increased with strain until strain at rupture ε. This occurred at 180% for native and 160% for DC Mesoderm tissue (Fig. 5A/B). Visually, rupture of fiber bundles was observed. Beyond this point, strength and tensile stress decreased with strain. Despite quantitative differences, this pattern was observed in all patient samples. Beyond 260% strain, the strength and tensile stress were similar again for native and DC tissue. Validity of test conditions in strips was confirmed by elongation of full vagina rings (Fig. 5C/D) and presented similar results of strength and tensile stress responses to strain.

Biomechanical assessment after DC presented a significantly decrease of the peak load (Fig. 5E, $0.01 < P < 0.05$), strain at rupture (Fig. 5F, $0.001 < P < 0.01$) and ultimate tensile stress (Fig. 5G, $0.01 < P < 0.05$). Elastic modulus E (the resistance to elastic deformation) (Fig. 5H) did not decrease significantly. Strength decreased by 55%, strain by 23%, stress by 55%, and elastic modulus by 68%.

Major constitutive ECM proteins retained after DC

Assessment of constitutive ECM proteins showed that Laminin-1/2 was mainly found around superior layers of the vaginal epithelium in both native vagina rings and after DC (Fig. 6). The Fibronectin-I/II/III (Fig. 7), Collagen-I (Fig. 8), and Ficolin-2B (Fig. 9) matrix proteins were evenly dispersed throughout the ECM. Despite an immunofluorescent signal decrease, Laminin was mostly retained after DC and Fibronectin was fully retained. Therefore, the chemical decellularization process of vaginal tissue had no major damaging effect on the ECM and its constitutive proteins. Collagen-I and Ficolin-2B were found to be present although (slightly) reduced after DC. This indicates minor chemical damage to (parts of) the ECM, induced by the DC process.

Discussion

Results

About 100 vaginoplasties on mostly patients with gender dysphoria and MRKHS are performed annually in our medical center[36,37]. However, complications arise from lack or absence of tissue, incompatibility of heterotopic autologous flaps/grafts and immunorejection of allogenic flaps. Immunogenicity can be prevented by decellularization, whilst preserving structural proteins and tissue structure for functionality and biocompatibility. Our study showed successful decellularization of human vaginal

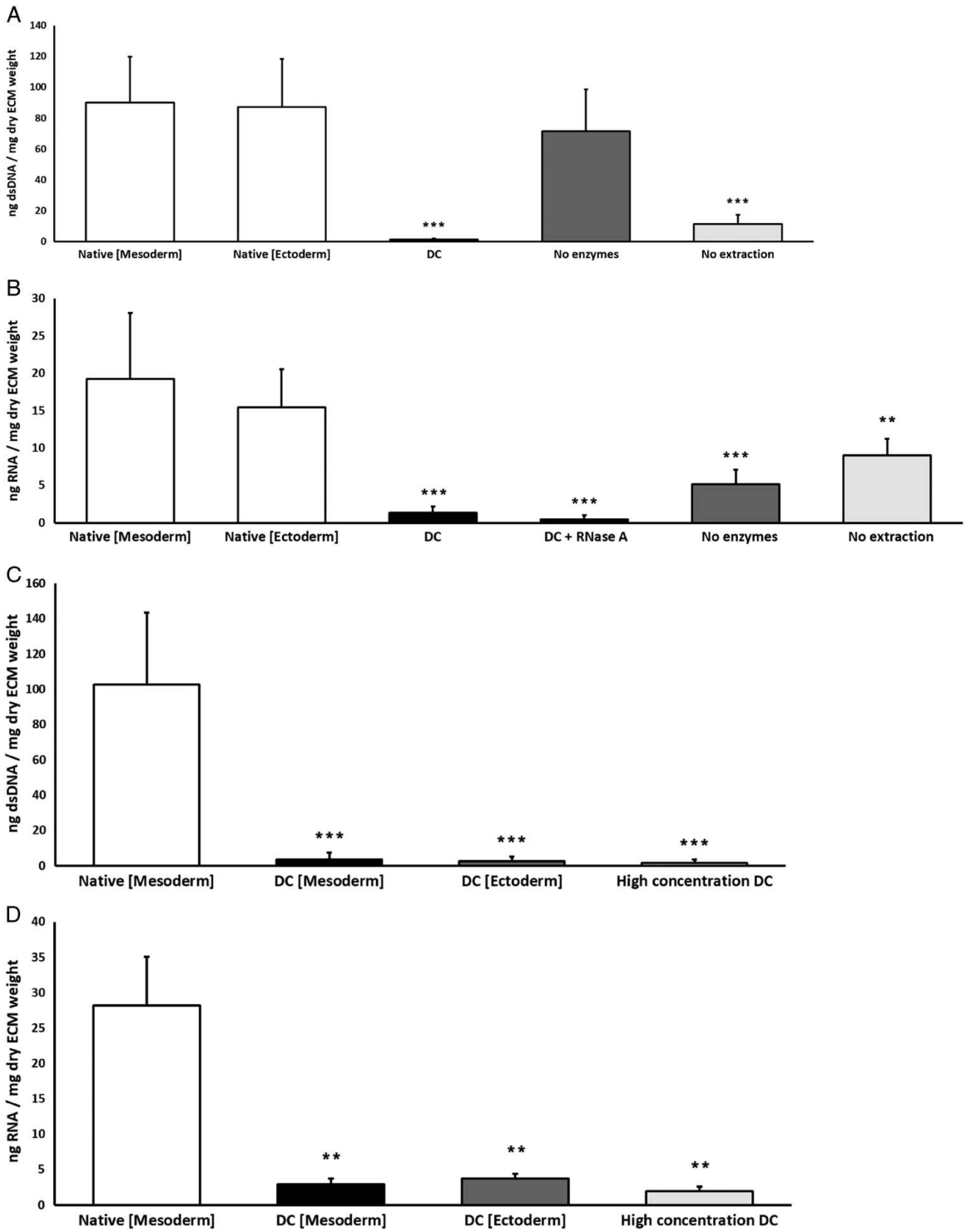

Figure 4. (A) Quantification of residual dsDNA, summarized as ng dsDNA/mg dry extracellular matrix weight. Concentration of dsDNA is significantly ($P < 0.001$) decreased in decellularized (DC) vaginal tissue and partial (DC) vaginal tissue with enzymatic degradation (no extraction) compared to native mesoderm and native ectoderm controls. (B) Quantification of residual RNA, summarized as ng RNA/mg dry extracellular matrix weight. Concentration of RNA is significantly ($P < 0.001$) decreased in DC vaginal tissue and partial DC vaginal tissue with membrane disruption (no enzymes) compared to native mesoderm and ectoderm controls. The data represents the means of seven experiments with SD. (C) Concentration of dsDNA is significantly ($P < 0.001$) decreased in decellularized full intact vaginal tissue rings from mesoderm (DC Mesoderm) and ectoderm (DC Ectoderm) sections and for decellularization with high chemical concentrations (High concentration DC). (D) Concentration of RNA is significantly ($P < 0.01$) decreased in decellularized full intact vaginal tissue rings from mesoderm (DC Mesoderm) and ectoderm (DC Ectoderm) sections and for decellularization with high chemical concentrations (High concentration DC). Significance is depicted with $^{*}P < 0.05$, $^{**}P < 0.01$, and $^{***}P < 0.001$.

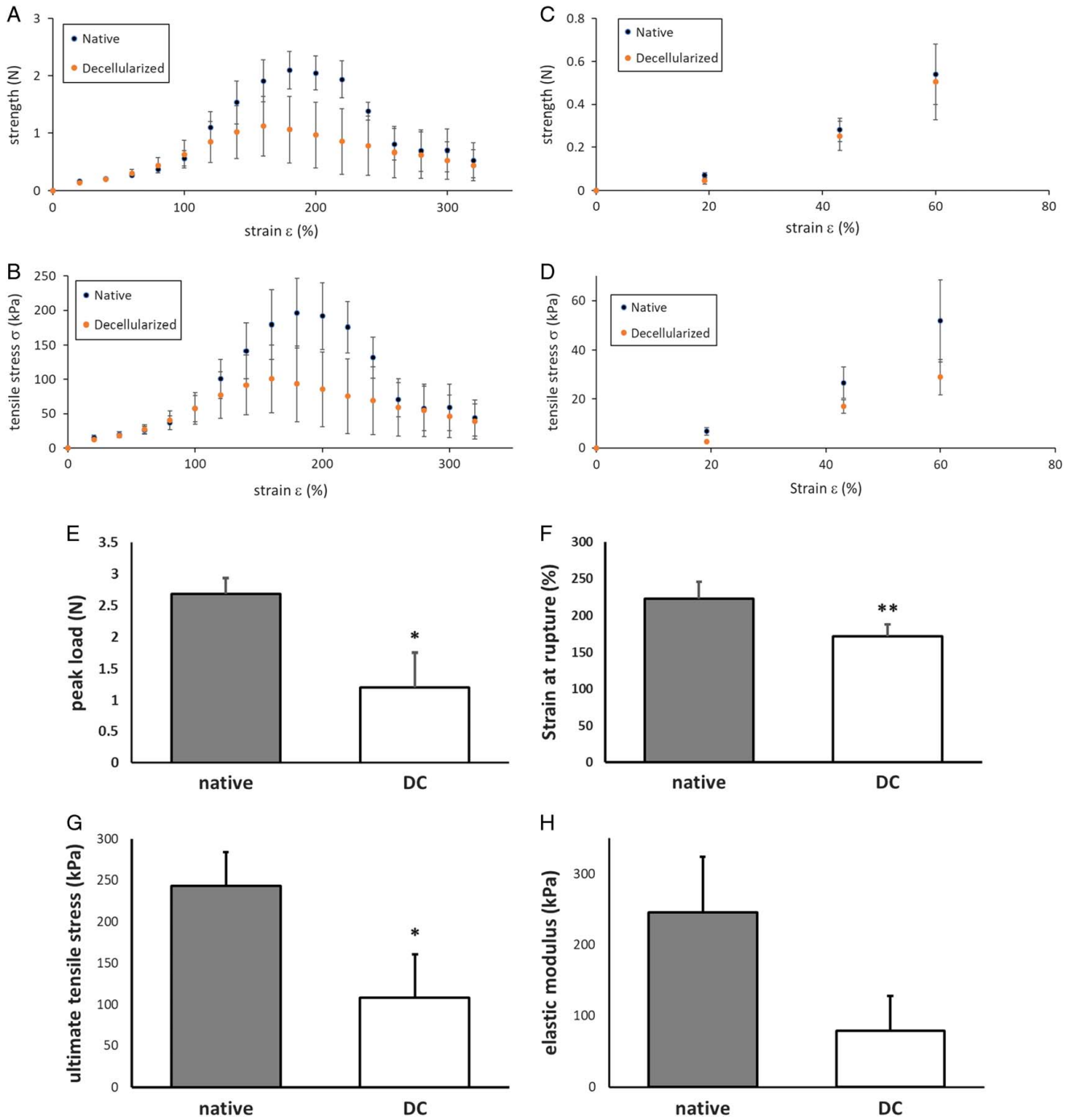

Figure 5. Mechanical properties of human native and decellularized (DC) vaginal tissue. (A) Force as function of strain for human vaginal tissue strips in Bioreactor. (B) Tensile stress σ as function of strain for human vaginal tissue strips in Bioreactor. (C) Force as function of strain for human full vaginal rings in Ring stretcher. (D) Tensile stress σ as function of strain for human full vaginal rings in Ring stretcher. The data represents the means of seven experiments. Mechanical properties of human native and DC vaginal tissue, measured with tissue strips in Bioreactor. (E) Peak load F_{max} 2.7 ± 0.2 N for native and 1.2 ± 0.6 N for DC tissue. (F) Strain at rupture ε_{rup} 223 ± 24% for native and 171 ± 17% for DC tissue. (G) Ultimate tensile stress σ_{ult} 244 ± 40 kPa for native and 108 ± 53 kPa for DC tissue. (H) Elastic modulus E 246 ± 77 N for native and 79 ± 49 kPa for DC tissue. The data represents the means of seven experiments with SEM. Significance is depicted with $^{*}P < 0.05$, $^{**}P < 0.01$, and $^{***}P < 0.001$.

tissue, based on commonly applied guidelines for acellular material: 1) absence of visible nuclei, 2) dsDNA quantity less than 50 ng AND less than 10%/mg dry ECM weight, and 3) remnant DNA fragments less than 200 bp.

Decellularization fully removed visible nuclei in vaginal mesoderm and ectoderm tissue with DAPI- and H&E-staining. Furthermore, DC caused no chemically induced loss of structural features. Partial DC by membrane disruption was incapable of

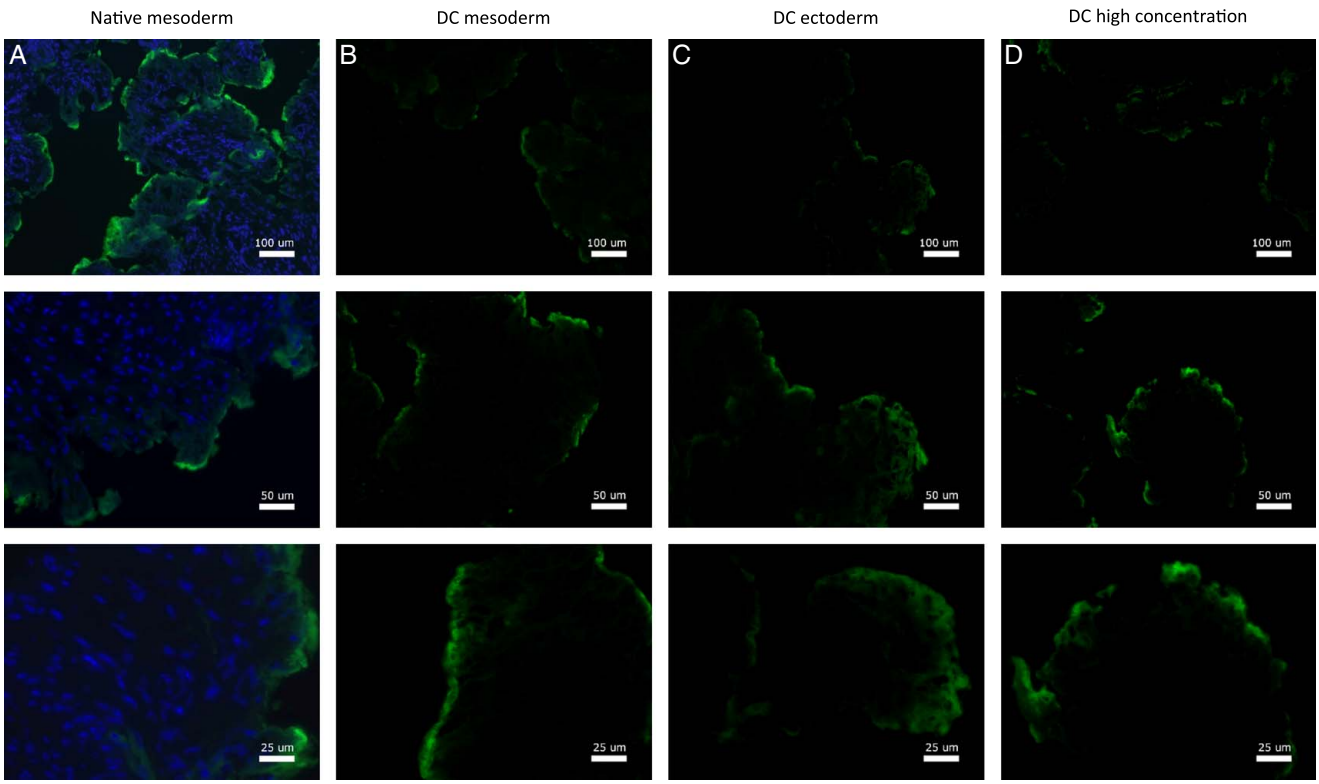

Figure 6. Fluorescence microscopy imaging of Laminin for vagina wall rings from (A) native, (B) decellularized mesoderm, (C) decellularized ectoderm, and (D) high-concentration decellularized mesoderm tissue. Fluorescence microscopy of Laminin was performed on and evaluated for all seven patient samples.

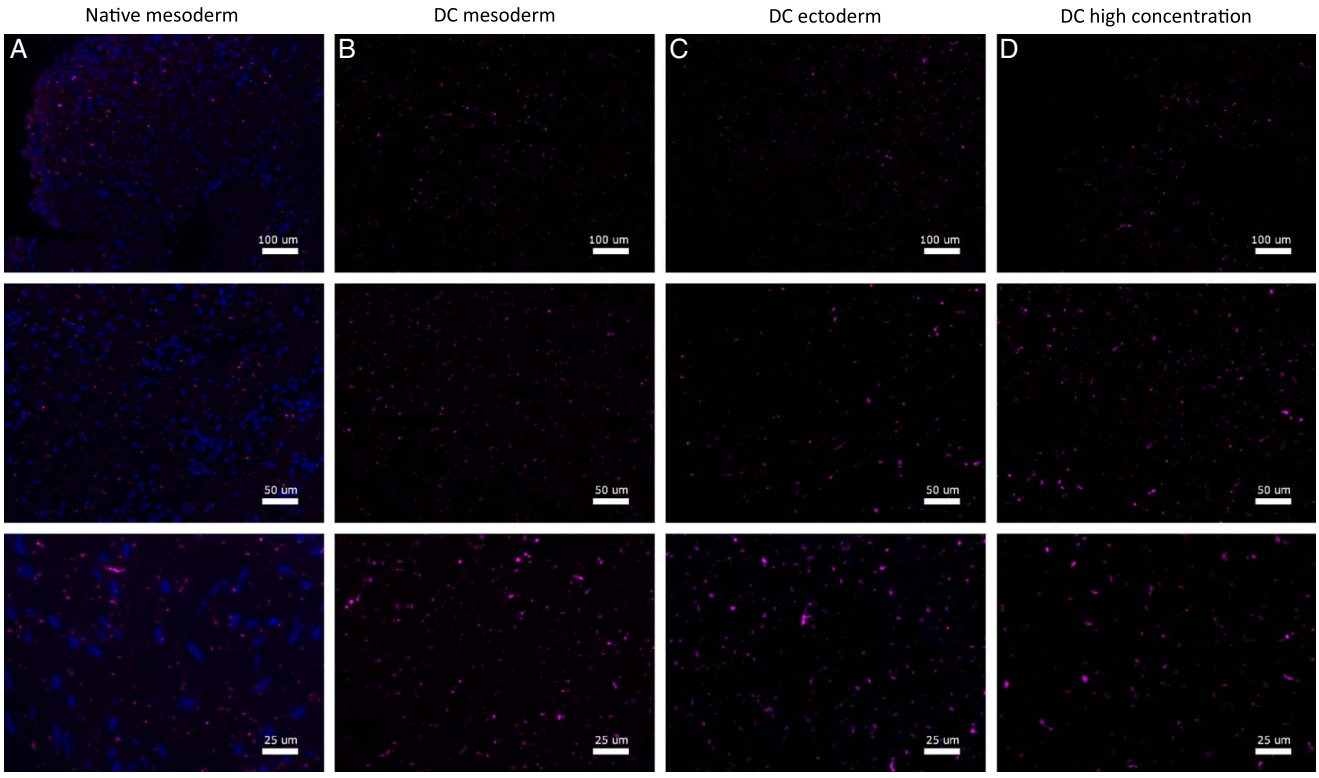

Figure 7. Fluorescence microscopy imaging of Fibronectin for vagina wall rings from (A) native, (B) decellularized mesoderm, (C) decellularized ectoderm, and (D) high-concentration decellularized mesoderm tissue. Fluorescence microscopy of Fibronectin was performed on and evaluated for all seven patient samples.

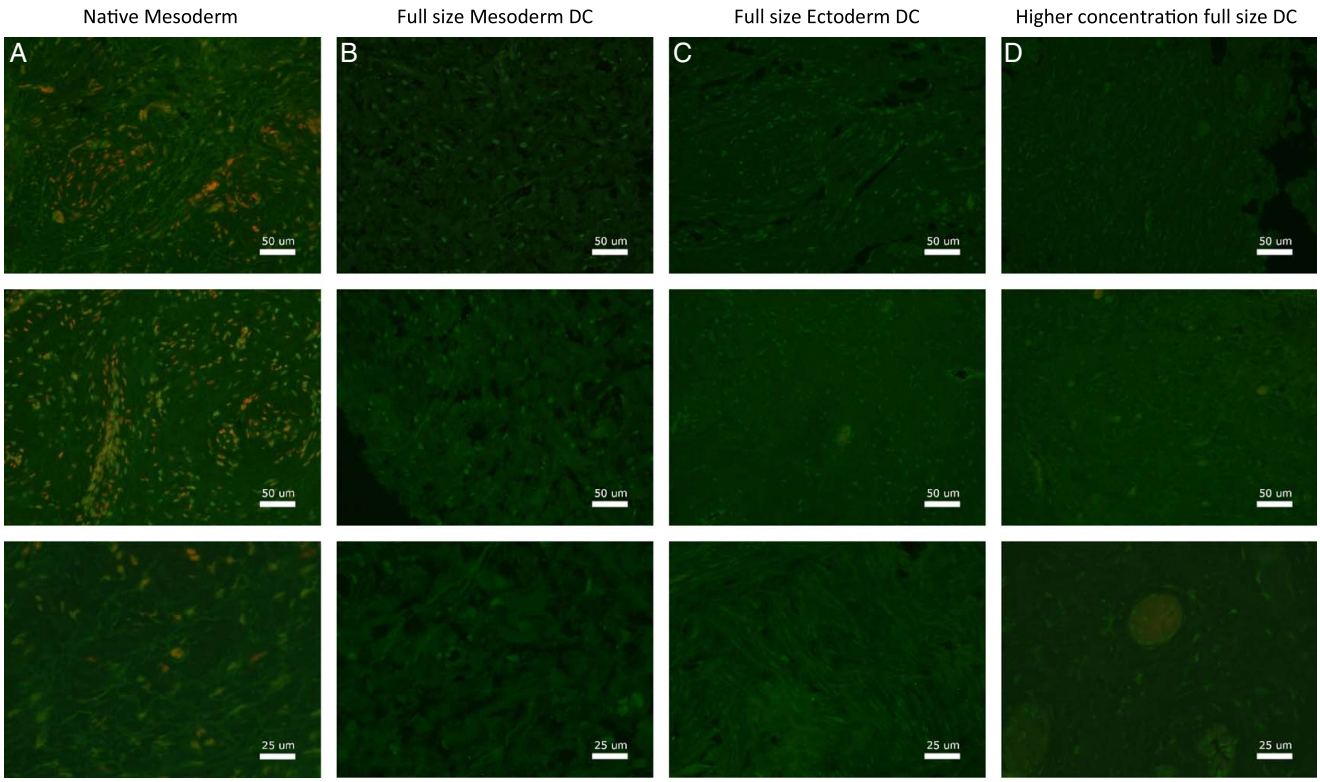

Figure 8. Fluorescence microscopy imaging of Collagen-I for vagina wall rings from (A) native, (B) decellularized mesoderm, (C) decellularized ectoderm, and (D) high-concentration decellularized mesoderm tissue. Fluorescence microscopy of Collagen-I was performed on and evaluated for all seven patient samples.

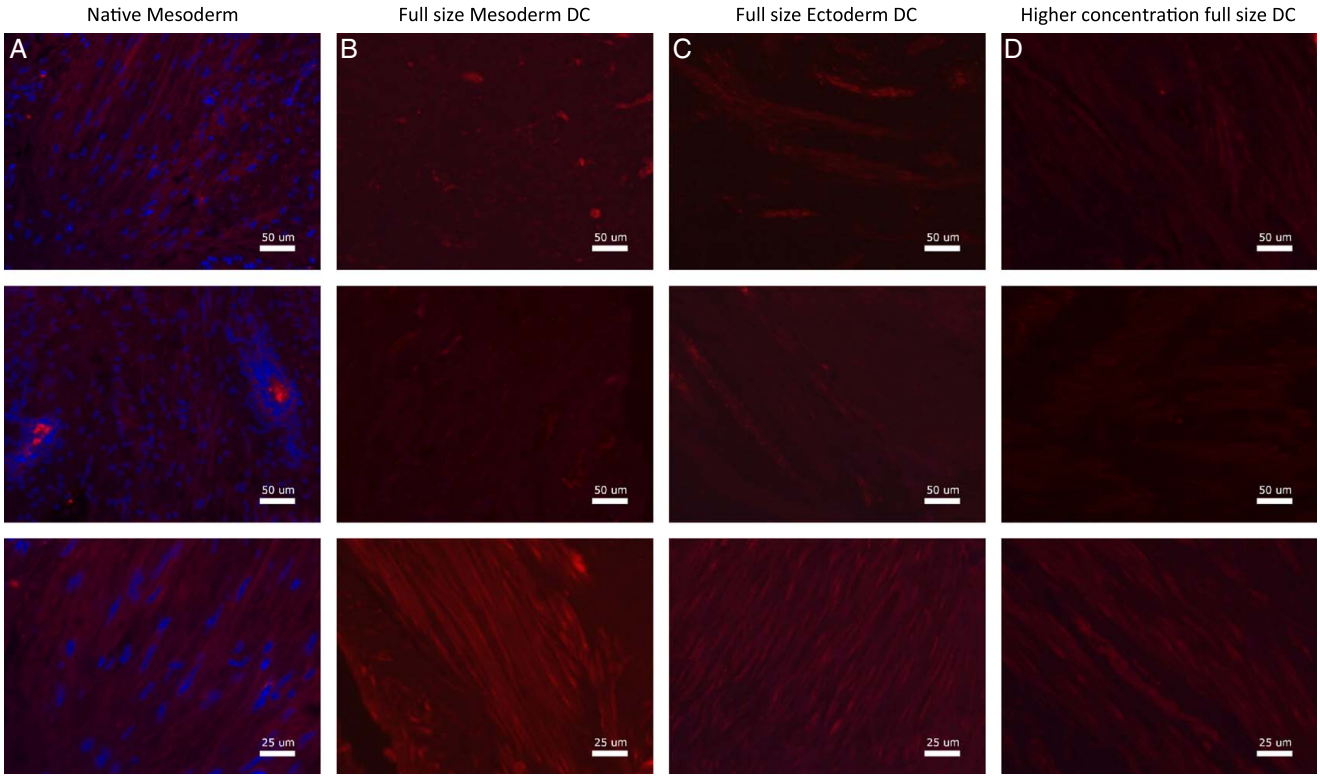

Figure 9. Fluorescence microscopy imaging of Ficolin for vagina wall rings from (A) native, (B) decellularized mesoderm, (C) decellularized ectoderm, and (D) high-concentration decellularized mesoderm tissue. Fluorescence microscopy of Ficolin was performed on and evaluated for all seven patient samples.

satisfactional DNA and RNA removal and partial DC by enzymatic degradation caused structural alteration.

Decellularization significantly reduced ($P < 0.001$) DNA concentrations to less than 50 ng AND less than 10%/mg dry ECM weight with lengths less than 200 bp. DC also significantly reduced RNA quantity ($P < 0.01$). Partial DC by membrane disruption was incapable of successful DNA removal but significantly reduced RNA quantity with successful DNA fragmentation. Partial DC by enzymatic degradation was incapable of successful DNA fragmentation but significantly reduced dsDNA quantity.

These findings indicates that both enzymatic degradation and membrane disruption play an essential role in successful DC of human vaginal matrix. DNA mobility decreases with length and depends on immobilization, random diffusion, active transport, anomalous subdiffusion, confined diffusion, transient confinement, and binding–unbinding mechanisms[38,39]. Short cytoplasmic DNA (<240 bp) is highly mobile through fast active transport and binding–unbinding[39], long DNA moves by slow anomalous subdiffusion and molecular crowding and nuclear DNA is almost immobile[38,39]. Membrane disruption breaks the cellular membrane[40], thus removes mitochondrial DNA (and cytoplasmic RNA), but nuclear DNA requires enzymatic fragmentation for mobilization to allow diffusion. At the same time, DNA fragmentation by enzymatic degradation relies on membrane disruption (likely by improving accessibility) for success.

According to the commonly applied acellular criteria[41], decellularization of human vaginal tissue was successful. However, these criteria only assess cellular material contamination based on DNA. DNA differs from other intracellular and extracellular components (including RNA, proteins, amino acids, lipids, and glycosaminoglycans) in physiology and chemistry and thus also their interaction with decellularization agents[41]. In our opinion, assessment of DC should always be supplemented with evaluation of tissue structure and function. As criteria on these aspects are nonexistent, we supplemented the definition of successful decellularization with: 4) visible structural features, 5) biocompatibility during stretching, and 6) presence of visible collagen, elastin, laminin and fibronectin. Our study also showed successful DC based on tissue structure and function, with space for improvement on biocompatibility and preservation of collagen and elastin.

Vaginal tissue structures were preserved with our DC protocol. However, enzymatic degradation caused structural alterations by nonextracted, fragmented DNA and other cellular waste components that build up after a 5-day partial DC with incomplete removal. DC with twice the original chemical concentrations induced structural changes. Many DC methods are known to cause structural damage[31,40] and should be avoided. Previously, induced structural alterations have been reported as prostatic metaplasia in seven FtM patients (18–34 years) after 24–72 months of exposure to testosterone cypionate and metastatic glands located predominantly in epithelial layers[42] or as 80% atrophy, 40% urothelial metaplasia, and 70% prostate-like glands in 10 FtM patients (22–74 years) after 2–10 years of androgen receival[43]. Although our included donors were presurgically exposed to testosterone for 2–11 (mean = 5.9) years, our samples did not present vaginal atrophy or prostatic metaplasia.

Of the ECM constituents, Laminin-I/II and Fibronectin-I/II/III were visibly retained and Collagen-I and Ficolin-2B were reduced after DC. Furthermore, DC reduced pull strength ($P < 0.05$), strain at rupture ($P < 0.01$), ultimate tensile stress ($P < 0.05$), and elastic modulus. Native and DC tissue had similar responses up to strain = 100%, corresponding to a pull strength of 0.6 N and 58 kPa tensile stress. Therefore, DC tissue is compatible under daily activity-like conditions, for which 40 kPa pressure at rest and 60 kPa contraction pressure[44] as well as 15% strain from smooth muscle contractions during sex are reported[45]. Mechanical strength is inhibited by cavities, loss of osmotic pressure after cell removal from the matrix[46] and weakening of the matrix after removal of muscle cells and proposedly by damaged collagen crosslinks[47]. This correlates with the observed visible reduction of collagen and elastin after DC. Tensile properties are inhibited by loss of proteoglycans or fibronectin. Fibronectin-I/II/III was found retained, but Proteoglycan is reportedly reduced by DC[20]. Furthermore, the reduced strain at rupture (157%) after DC is comparable to premenopausal control groups[48]. As strength and elasticity dependent on expression of multiple ECM proteins, the observed decrease can therefore be explained by the visible reduction of Collagen-I and Ficolin-2B[49,50].

Future prospective

Successful reconstruction of a vagina for future clinical applications will depend upon a suitable matrix, the viability thereof and the availability of autologous cells to repopulate the biomaterial. It is now possible to create an appropriate matrix from readily available human donor tissue. However, this DC vaginal matrix, at a clinically relevant vagina size, exceeds the diffusion limit and thus needs active transport of oxygen and nutrients. Our current follow-up study involves imaging of the vagina vasculature and confirms the (partial) preservation of vessels and veins after DC. We are confident that by recolonization of the vaginal matrix with autologous host cells, the incorporated neovascularization will allow for tissue survival and recellularization will improve biocompatibility through collagen and elastin restoration. Other aspects that are crucial for successful vagina transplantation are matrix sterility, isolation, and expansion of autologous cells and (long term) implant safety.

Conclusion

Our study confirmed that the multistep DC protocol is effective to prepare acellular vaginal tissue from healthy full human donor flaps, with retained structure, sufficient biomechanical properties and (partial to full) conservation of structural proteins. This is a promising biomaterial for vaginal reconstruction, as the orthotopic origin should increase functionality by reducing complications associated with nonvaginal tissue. Our DC protocol is successful for vaginal tissue, but is applicable to any type of (human) tissue after optimization of chemical concentrations. However, restoration of collagen and elastin is vital for required biomechanical properties, like stiffness and strength as a hollow organ, and flexibility during sex and in natural child birth. Lastly, the potential of our DC protocol for future vagina transplantation, transcends donation from transgender individuals and is applicable to tissue from healthy, deceased donors as well.

Ethical approval

Ethical approval was given by the institutional Medical Ethical Examination Committee of Amsterdam UMC location VU Medical Center (Amsterdam; IRB approval by METc VUmc registration number 2018/3190, October 2018). Tissue collection and experimental usage was approved by the institutional Medical Ethical Examination Committee. Patient consent for tissue donation and experimental usage was obtained and documented prior to surgery and participation had no positive or negative effect on their treatment.

Consent

Written informed consent was obtained from patients for publication and any accompanying images. A copy of the written consent is available for review by the Editor-in-Chief of this journal on request.

Sources of funding

This research did not receive any specific grant from funding agencies in the public, commercial, or not-for-profit sectors.

Author contribution

J.S.: conceptualization, data collection, data analysis and interpretation, writing – original draft. F.X.: conceptualization, data collection, data interpretation, writing – review and editing. J.-P.R. and M.-B.B.: writing – review and editing. F.G. and J.H.: conceptualization, data interpretation, writing – review and editing. H.M.: conceptualization, data collection, data analysis, writing – review and editing. T.S.: conceptualization, data analysis, data interpretation writing – review and editing.

Conflicts of interest disclosure

There are no conflicts of interest.

Research registration unique identifying number (UIN)

Not applicable.

Guarantor

Professor Dr Judith Huirne.

Data availability statement

The raw/processed data required to reproduce these findings cannot fully be shared at this time as the data also forms part of an ongoing study. However, data can be shared upon request from the corresponding author.

Provenance and peer review

Not invited.

Acknowledgements

The authors would like to thank Remco Keijzer, Saskia van Daalen, Cindy de Winter-Korver, Wendy Noort, and Zeliha Güler for their assistance with the study.

References

[1] Callens N, De Cuypere G, Wolffenbuttel KP, *et al*. Long-term psychosexual and anatomical outcome after vaginal dilation or vaginoplasty: a comparative study. J Sex Med 2012;9:1842–51.
[2] Herlin M, Bjørn AMB, Rasmussen M, *et al*. Prevalence and patient characteristics of Mayer-Rokitansky-Küster-Hauser syndrome: a nationwide registry-based study. Hum Reprod 2016;31:2384–90.
[3] Liao LM, Doyle J, Crouch NS, *et al*. Dilation as treatment for vaginal agenesis and hypoplasia: a pilot exploration of benefits and barriers as perceived by patients. J Obstet Gynaecol (Lahore) 2006; 26:144–8.
[4] Callens N, Weyers S, Monstrey S, *et al*. Vaginal dilation treatment in women with vaginal hypoplasia: a prospective one-year follow-up study. Am J Obstet Gynecol 2014;211:228–29. e1-e12.
[5] Cheikhelard A, Bidet M, Baptiste A, *et al*. Surgery is not superior to dilation for the management of vaginal agenesis in Mayer-Rokitansky-Küster-Hauser syndrome: a multicenter comparative observational study in 131 patients. Am J Obstet Gynecol 2018;219:281.e1–9.
[6] Wiepjes CM, Nota NM, de Blok CJM, *et al*. The Amsterdam Cohort of Gender Dysphoria Study (1972–2015): trends in prevalence, treatment, and regrets. J Sex Med 2018;15:582–90.
[7] Buncamper ME, Honselaar JS, Bouman MB, *et al*. and functional outcomes of neovaginoplasty using penile skin in male-to-female transsexuals. J Sex Med [Internet] 2015;12:1626–34.
[8] Hess J, Neto RR, Panic L, *et al*. Satisfaction with male-to-female gender reassignment surgery – results of a retrospective analysis. Dtsch Arztebl Int 2014;111:795–801.
[9] Van Der Sluis WB, Bouman MB, Meijerink WJHJ, *et al*. Diversion neovaginitis after sigmoid vaginoplasty: endoscopic and clinical characteristics. Fertil Steril 2016;105:834–39.e1.
[10] Bouman MB, van der Sluis WB, van Woudenberg Hamstra LE, *et al*. Patient-reported esthetic and functional outcomes of primary total laparoscopic intestinal vaginoplasty in transgender women with penoscrotal hypoplasia. J Sex Med 2016;13:1438–44.
[11] Pusic AL, Mehrara BJ. Vaginal reconstruction: an algorithm approach to defect classification and flap reconstruction. J Surg Oncol 2006;94: 515–21.
[12] Panici PB, Ruscito I, Gasparri ML, *et al*. Vaginal reconstruction with the Abbè-McIndoe technique: from dermal grafts to autologous in vitro cultured vaginal tissue transplant. Semin Reprod Med 2011; 29:45–54.
[13] Cadili A, Kneteman N. The role of macrophages in xenograft rejection. Transplant Proc 2008;40:3289–93.
[14] Dorin RP, Atala A, Defilippo RE. Bioengineering a vaginal replacement using a small biopsy of autologous tissue. Semin Reprod Med 2011;29: 38–44.
[15] Buncamper ME, Van Der Sluis WB, Van Der Pas RSD, *et al*. Surgical outcome after penile inversion vaginoplasty: a retrospective study of 475 transgender women. Plast Reconstr Surg 2016;138:999–1007.
[16] van der Sluis WB, Bouman MB, de Boer NKH, *et al*. Long-term follow-up of transgender women after secondary intestinal vaginoplasty. J Sex Med 2016;13:702–10.
[17] Sueters J, Groenman FA, Bouman M-B, *et al*. Tissue engineering neovagina for vaginoplasty in MRKHS and GD patients – a systematic review. Tissue Eng Part B Rev 2022;28:1–23.
[18] Rabin RC. Doctors transplant ear of human cells, made by 3-d printer. The New York. Times 2022:1.
[19] Rafat M, Jabbarvand M, Sharma N, *et al*. Bioengineered corneal tissue for minimally invasive vision restoration in advanced keratoconus in two clinical cohorts. Nat Biotechnol 2022;40:1–22.
[20] Greco KV, Jones LG, Obiri-Yeboa I, *et al*. Creation of an acellular vaginal matrix for potential vaginal augmentation and cloacal repair. J Pediatr Adolesc Gynecol 2018;31:473–9.
[21] Ho MH, Heydarkhan S, Vernet D, *et al*. Stimulating vaginal repair in rats through skeletal muscle-derived stem cells seeded on small intestinal submucosal scaffolds. Obstet Gynecol 2009;114:300–9.

[22] Ding JX, Chen LM, Zhang XY, *et al*. Sexual and functional outcomes of vaginoplasty using acellular porcine small intestinal submucosa graft or laparoscopic peritoneal vaginoplasty: a comparative study. Hum Reprod 2015;30:581–9.
[23] Zhang JK, Du RX, Zhang L, *et al*. A new material for tissue engineered vagina reconstruction: acellular porcine vagina matrix. J Biomed Mater Res - Part A 2017;105:1949–59.
[24] De Filippo RE, Bishop CE, Filho LF, *et al*. Tissue engineering a complete vaginal replacement from a small biopsy of autologous tissue. Transplantation 2008;86:208–14.
[25] Hou C, Zheng J, Li Z, *et al*. Printing 3D vagina tissue analogues with vagina decellularized extracellular matrix bioink. Int J Biol Macromol 2021;180:177–86.
[26] Wefer J, Sekido N, Sievert KD, *et al*. Homologous acellular matrix graft for vaginal repair in rats: a pilot study for a new reconstructive approach. World J Urol 2002;20:260–3.
[27] Li N, Huang R, Zhang X, *et al*. Stem cells cardiac patch from decellularized umbilical artery improved heart function after myocardium infarction. Biomed Mater Eng 2017;28(s1):S87–94.
[28] Ruiz-Zapata AM, Heinz A, Kerkhof MH, *et al*. Extracellular matrix stiffness and composition regulate the myofibroblast differentiation of vaginal fibroblasts. Int J Mol Sci 2020;21:1–15.
[29] Nikkels C, van Trotsenburg M, Huirne J, *et al*. Vaginal colpectomy in transgender men: a retrospective cohort study on surgical procedure and outcomes. J Sex Med 2019;16:924–33.
[30] Brown BN, Valentin JE, Stewart-Akers AM, *et al*. Macrophage phenotype and remodeling outcomes in response to biologic scaffolds with and without a cellular component. Biomaterials 2009;30:1482–91.
[31] Crapo PM, Gilbert TW, Badylak SF. An overview of tissue and whole organ decellularization processes. Biomaterials 2011;32:3233–43.
[32] Groenman F, Nikkels C, Huirne J, *et al*. Robot-assisted laparoscopic colpectomy in female-to-male transgender patients; technique and outcomes of a prospective cohort study. Surg Endosc 2017;31:3363–9.
[33] Mabuchi T, Nishikawa S. Selective staining with two fluorochromes of DNA fragments on gels depending on their AT content. Nucleic Acids Res 1990;18:7461–2.
[34] Kapuscinski J, Yanagi K. Selective staining by 4', 6-diamidine-2-phenylindole of nanogram quantities of DNA in the presence of RNA on gels. Nucleic Acids Res 1979;6:3535–42.
[35] Sicari BM, Johnson SA, Siu BF, *et al*. The effect of source animal age upon the in vivo remodeling characteristics of an extracellular matrix scaffold. Biomaterials 2012;33:5524–33.
[36] Van Der Sluis WB, De Nie I, Steensma TD, *et al*. Surgical and demographic trends in genital gender-affirming surgery in transgender women: 40 years of experience in Amsterdam. Br J Surg 2022;109:8–11.
[37] Leemrijse C, Dulmen S Van. Genitale operaties bij kinderen met DSD, Nivel. 2023; ISBN 978-94-6122-769-0.
[38] Lukacs GL, Haggie P, Seksek O, *et al*. Size-dependent DNA mobility in cytoplasm and nucleus. J Biol Chem 2000;275:1625–9.
[39] Mieruszynski S, Digman MA, Gratton E, *et al*. Characterization of exogenous DNA mobility in live cells through fluctuation correlation spectroscopy. Sci Rep 2015;5(February):1–10.
[40] Gilbert TW, Sellaro TL, Badylak SF. Decellularization of tissues and organs. Biomaterials 2006;27:3675–83.
[41] Aamodt JM, Grainger DW. Extracellular matrix-based biomaterial scaffolds and the host response. Biomaterials 2016;86:86–2.
[42] Anderson WJ, Kolin DL, Neville G, *et al*. Prostatic metaplasia of the vagina and uterine cervix: an androgen-associated glandular lesion of surface squamous epithelium. Am J Surg Pathol 2020;44:1040–9.
[43] Dasaraju S, Klein ME, Murugan P, *et al*. Microscopic features of vaginectomy specimens from transgender patients. Am J Clin Pathol 2022;158:639–45.
[44] Egorov V, Murphy M, Lucente V, *et al*. Quantitative assessment and interpretation of vaginal conditions. Sex Med 2018;6:39–48.
[45] Huntington A, Abramowitch SD, Moalli PA, *et al*. Strains induced in the vagina by smooth muscle contractions. Acta Biomater 2021;129:178–87.
[46] Schleifenbaum S, Prietzel T, Aust G, *et al* Acellularization-Induced changes in tensile properties are organ specific - An In-Vitro mechanical and structural analysis of porcine soft tissues. PLoS One. 2016:11. doi:10.1371/journal.pone.0151223
[47] Schleifenbaum S, Prietzel T, Aust G, *et al*. Acellularization-induced changes in tensile properties are organ specific – an in-vitro mechanical and structural analysis of porcine soft tissues. PLoS One 2016;11:e0151223.
[48] Lei L, Song Y, Chen RQ. Biomechanical properties of prolapsed vaginal tissue in pre- and postmenopausal women. Int Urogynecol J 2007;18:603–7.
[49] Goh JTW. Biomechanical and biochemical assessments for pelvic organ prolapse. Curr Opin Obstet Gynecol 2003;15:391–4.
[50] Petros PE, Ulmsten UI. An integral theory of female urinary incontinence. Experimental and clinical considerations. Acta Obs gynecol scand suppl 1990;69:7–31.